Mater. Res. Soc. Symp. Proc. Vol. 1720 © 2015 Materials Research Society
DOI: 10.1557/opl.2015.293

Green Synthesis of $Y_2O_3:Eu^{3+}$ Nanocrystals for Bioimaging

Adrine Malek Khachatourian[1,2], Farhad Golestani-Fard[2], Hossein Sarpoolaky[2], Carmen Vogt[3], Yichen Zhao[1], Muhammet S. Toprak[1].
[1]Department of Materials and Nano Physics, KTH-Royal Institute of Technology, SE 16440 Kista-Stockholm, Sweden.
[2]School of Metallurgy and Materials Engineering, IUST-Iran University of Science and Technology, 16846 Tehran, Iran.
[3]Department of Biomedical and X-ray Physics, KTH-Royal Institute of Technology, 10044 Stockholm, Sweden.

ABSTRACT

Rare earth (e.g., Eu, Er, Yb, Tm) doped Y_2O_3 nanocrystals are promising fluorescent bioimaging agents which can overcome well known problems of currently used organic dyes like photobleaching, phototoxicity, and light scattering. Furthermore, the alternative quantum dots (QDs) composed of heavy metals (e.g., CdSe) possess inherently low biocompatibility due to the heavy metal content. In the present work, monodisperse spherical $Y_2O_3:Eu^{3+}$ nanocrystals were successfully synthesized by microwave assisted urea precipitation method followed by thermochemical treatment. This is a green, fast and reproducible synthesis method, which is surfactant and hazardous precursors free. The as prepared particles were non-aggregated, spherical particles with a narrow size distribution. The calcined particles have a polycrystalline structure preserving the monodispersity and the spherical morphology of the as prepared particles. After calcination of $Y(OH)CO_3:Eu^{3+}$ precursors at 900°C for 2 hours, a highly crystalline cubic Y_2O_3 structure was obtained. The $Y_2O_3:Eu^{3+}$ spherical particles showed a strong red emission peak at 613nm due to the $^5D_0$–$^7F_2$ forced electric dipole transition of Eu^{3+} ions under UV excitation (235 nm) as revealed by the photoluminescence analysis (PL). The effect of reaction time on size and photoluminescence properties of calcined particles and also the effect of reaction temperature and pressure on the size and the yield of the precipitation process have been studied. The intense red fluorescent emission, excellent stability and potential low toxicity make these QDs promising for applications in bio-related areas such as fluorescence cell imaging or fluorescence bio labels.

INTRODUCTION

Rare earth doped nanocrystalline Y_2O_3 luminescent materials have attracted interest for applications in display and lightening devices due to high luminescence quantum efficiency, superior chemical stability and color purity [1–3]. For these purposes a wide variety of colors is generated by doping different lanthanide ions in Y_2O_3 host matrix such as Eu^{3+} for red, Tb^{3+} for green, Tm^{3+} for blue and Dy^{3+} for yellow emission wavelengths [4]. Each dopant element has fixed and particle size independent emission wavelengths [5], the “caged atoms” in the host matrix create their own atomic levels within the band gap of the Y_2O_3 host material [6]. Recently these materials have attracted attention because of their potential applications in biomolecular detection, medical diagnostics, bio labels and bio imaging probes [5,7–10].

In the fluorescence bioimaging applications organic dyes were traditionally used. However because of short observation times as a result of photobleaching and low assay

sensitivity from broad absorption and emission bands, the organic dyes are lately replaced by semiconductor quantum dots (QDs) which are more stable against photobleaching, possess narrow emission band and size dependent tunable emission [11,12]. Though, due to the fact that most of these QDs are composed of toxic elements (Cd,Se,Pd,Te, and Hg), their long term uses have been limited due to concerns regarding the inherent cytotoxicity of these materials [11,13]. Furthermore, QDs are generally synthesized under expensive, time consuming and hazardous experimental conditions [5]. Rare earth doped Y_2O_3 nanocrystals are a promising alternative to QDs because of the nontoxic composition [13,14]. Characteristics including high quantum efficiency, superior photostability and biocompatibility, sharp emission and absorption bands and long life time make them attractive in bioimaging applications [5–7].

In this paper monodispersed $Y_2O_3:Eu^{3+}$ (9 mol %) red emitting nanocrystals were successfully synthesized by microwave assisted urea precipitation method and compared with particles synthesized by conventional method. This method is a green, fast, surfactant and hazardous precursors free and reproducible synthesis method. The effect of reaction temperature and pressure on the size and the yield of the precipitation process and also the effect of reaction time on size and photoluminescence properties of calcined particles have been investigated.

EXPERIMENT

$Y(NO_3)_3.6H_2O$ (Sigma-Aldrich 99.98%), $Eu(NO_3)_3.5H_2O$ (Sigma-Aldrich 99.99%) and urea (Merck ≥ 99%) were dissolved separately in deionized water (Millipore, 15 MΩ cm) to prepare stock solution of $Y(NO_3)_3$, $Eu(NO_3)_3$, and urea respectively. Then appropriate amount of these solutions were mixed together in septa sealed vials and then heated in Biotage® initiator laboratory microwave (Biotage, Uppsala, Sweden) at different temperatures for 5-30 min. The precipitates were collected by centrifugation at 8000 rpm and washed twice with deionized water and ethanol (Solveco 99.5%), followed by calcination at 900°C for 2h.

The synthesized particles have been characterized by Transmission electron microscopy (TEM) (JEOL JEM-2100F operating at an accelerating voltage of 200 kV, JEOL Ltd., Japan,), Scanning electron microscopy (SEM) (Gemini- Zeiss Ultra 55 FEG-SEM, Germany) equipped with an energy dispersive X-ray spectroscopy (EDS) for microstructure characterization and elemental mapping of the calcined powders, X-ray diffraction (XRD) (Philips PAN analytical X'Pert Pro powder diffractometer with Cu-Kα radiation, 45 kV, 40 mA, USA), Thermogravimetric analysis (TGA) (TGA-Q500, TA instruments, USA), and Photoluminescence spectroscopy (PL) (Perkin–Elmer LS 55 fluorescence spectrometer, Perkin Elmer, USA).

DISCUSSION

In our previous study [15] the effect of molar ratio of [urea]/[metal ions] (u) in microwave assisted synthesis of particles has been investigated. Using an u above 10 in the primary solution resulted in homogenous and monosized spherical particles and further increment in u decreased the size of the obtained particles. In the present work a comparison between microwave heating and conventional heating for the synthesis of $Y_2O_3:Eu^{3+}$ particles is performed. Solutions with concentration of metals ions $[Y^{3+} + Eu^{3+}] = 0.02$ M, u=30 and molar ratio of $[Y^{3+}]/[Eu^{3+}] = 10$ are prepared and heated in the microwave system at 90°C for 15 minutes and at 90°C for 2 hours by conventional heating in an oil bath under the reflux condition. The morphology of as prepared particles is analyzed by TEM (Figure 1). The

microwave synthesized powders are monodispersed, with a spherical morphology and a narrow size distribution (184 ± 17 nm) whereas the particles obtained by conventional heating are polydispersed (113 ± 158 nm). This is explained by fundamental differences between the microwave heating and conventional heating. In the microwave assisted urea precipitation method the solution is heated uniformly and internally within the liquid in very short times (less than 90 s). The rapid volumetric heating results in dramatic increase in reaction rates and rapid decomposition of large amount of urea followed by a burst of nucleation of particles and diffusion controlled growth of nuclei. In contrast, in the conventional heating process, heat is originating from external heating sources and results in a multistep nucleation and growth mechanism followed by Ostwald ripening. In conventional heating monodispersed particles can be obtained by longer reaction times (several hours) and higher urea concentration although the final particles have sub - micrometric sizes and are aggregated.

The effect of reaction temperature and pressure on the yield of the precipitation process is studied (Table 1). We maintain constant *u*, the metal ions concentration and the reaction time. By increasing the reaction temperature from 90°C to 185°C, the internal pressure over the sealed solution increases from 0 to 14 bar, the size of as prepared particles increases from 184 ± 17 nm to 483 ± 25 nm while the yield of the precipitation process improves significantly from 52 % to 93 %. The high efficiency of the process can be explained by accelerated kinetics of the decomposition and precipitation reactions in presence of higher temperature and pressure, under supercritical conditions. The increase in the particle size can be explained by increase in particles growth rate and increase in the reaction yield under higher temperature conditions and corresponding higher pressures.

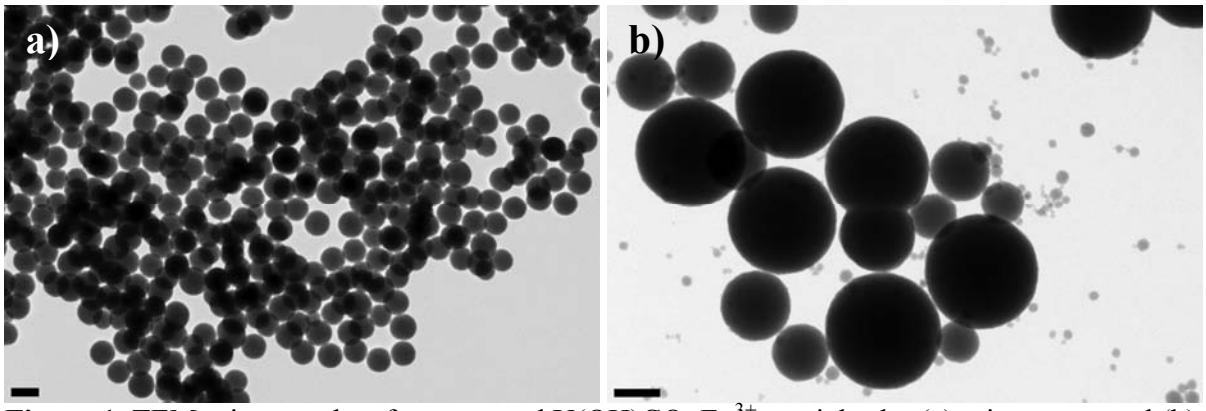

Figure 1. TEM micrographs of as prepared $Y(OH)CO_3{:}Eu^{3+}$ particles by (a) microwave and (b) conventional heating methods (the length of the scale bar represents 200 nm).

Table 1. The effect of reaction temperature and pressure on the yield of precipitation process.

Reaction temperature (°C)	90	100	120	150	165	185
Measured pressure (bar)	0	0.5	2	5	8	14
Yield of precipitation process (%)	52	63	80	89	93	92

The thermal decomposition process of the as prepared precursor is investigated by TGA measurements (Figure 2a). The total weight loss from 100 to 850°C is around 34%, which is due to evaporation of physically adsorbed water and the decomposition reactions of carbonates present in the precursor powder. The precursor fully converts to oxide form above 850°C.

Sordelet et al [16] described the decomposition mechanism previously. Shortly, the hydroxycarbonate precipitate obtained by conventional urea precipitation method underwent two-step decomposition and converted to oxide as shown by the reactions given below:

$2Y(OH)CO_3\ (s) \rightarrow Y_2O_2CO_3(s) + H_2O\ (g) + CO_2\ (g)$

$Y_2O_2CO_3(s) \rightarrow Y_2O_3(s) + CO_2\ (g)$

The as prepared particles and the calcined particles at 900°C for 2 h are analyzed by XRD (Figure 2b). All diffraction peaks in as prepared particles can be indexed to orthorhombic phase of $Y(OH)CO_3$ (JCPDS ref. no. 01-070-0278) while the calcined particles are highly crystalline cubic Y_2O_3 phase with no detectable impurity peaks (JCPDS ref. no. 01-073-1334). In XRD patterns the shift of the diffraction peaks' position to lower angles for calcined Y_2O_3:Eu^{3+} (9 mol %) particles in comparison to pure Y_2O_3 particles confirms the substitution of the dopant ions into the host crystal structure, based on the fact that the ionic radius of Eu^{3+} (0.109 nm) is larger than that of Y^{3+} (0.104 nm). For example the position of (222) plane shifts from 29.09° (Eu^{3+} 0%) to 29.02° (Eu^{3+} 13%). Additionally, regardless of the initial reaction temperature, all calcined particles at 900°C have cubic Y_2O_3 structure.

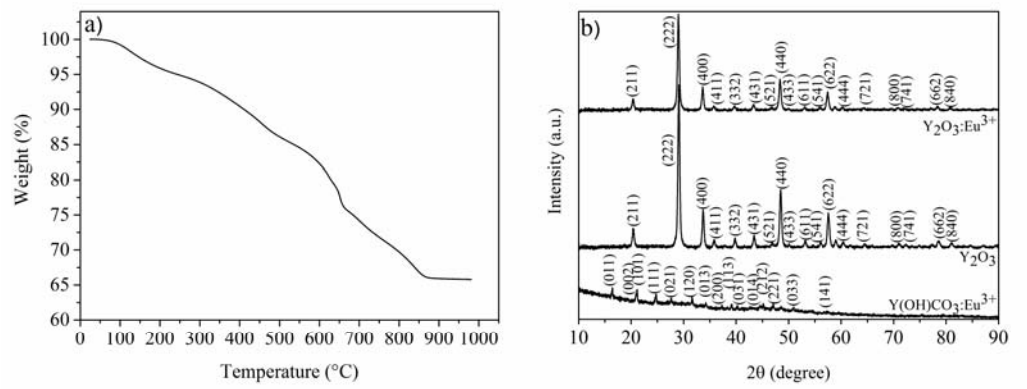

Figure 2. (a) TGA thermogram of as prepared particles, and (b) XRD patterns of the as prepared particles, doped and non-doped particles calcined at 900°C.

Furthermore, the effect of reaction time is investigated. For a fixed *u* of 30 and metal ions concentration of 0.02 M, when the reaction time increases from 5 to 30 minutes the size of particles slightly increases from 175 ± 18 nm to 210 ± 21 nm, whereas the yield of the process does not change significantly. It is notable that even for 5 minutes reaction time a stable suspension is formed. All particles after calcination at 900°C have cubic Y_2O_3 structure and the peaks in XRD patterns become sharper with the increase of reaction time (data not shown).

The PL properties of the calcined particles under the UV excitation (235 nm) are studied (Figure 3a). The emission peaks observed in the spectrum are due to transitions from $^5D_0$ level to ^7F_J (J=0, 1, 2, …) levels of Eu^{3+} ions in the cubic Y_2O_3 host crystal [17]. All particles exhibit a strong red emission peak centered at 613 nm, which becomes more intense as the reaction temperature increased. The increased PL intensity is probably due to higher crystallinity of the particles at longer reaction times.

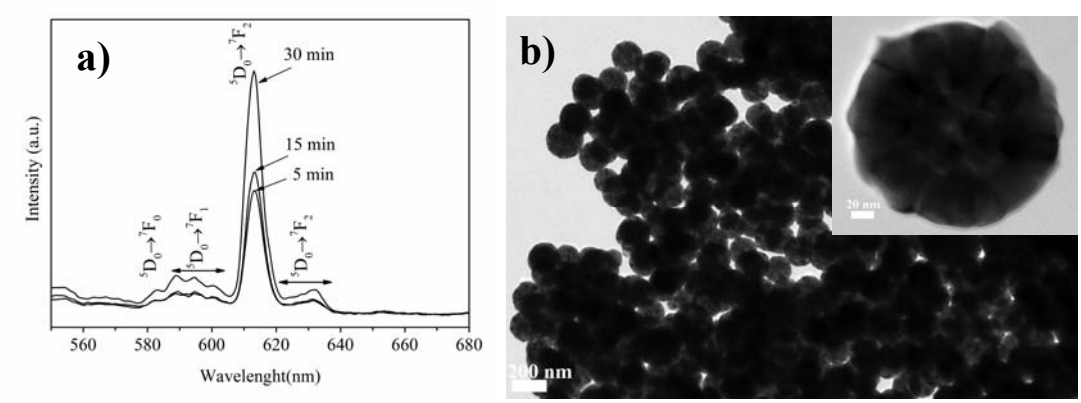

Figure 3. (a) PL spectrum of calcined Y_2O_3:Eu^{3+} particles synthesized with different reaction times (5 min, 15 min and 30 min) and (b) TEM micrograph of Y_2O_3:Eu^{3+} particles calcined at 900°C for 2h.

The morphology of the calcined particles is further analyzed by TEM and SEM. The calcined particles display a polycrystalline structure (inset Figure 3b) containing small crystallites with an average size of ~35 nm. The monodispersity and spherical morphology of the as prepared particles is maintained even after calcination at high temperature (Figure 3b and Figure 4). Elemental mapping of Eu and Y elements by EDS also confirms the homogenous distribution of Eu^{3+} ions in Y_2O_3 structure (Figure 4). The homogeneous distribution of Y (green color) in the particles in Fig 4b corroborates the XRD data of Y_2O_3 structure while Eu (red color) in Fig 4c is homogeneous but less dominantly distributed in the Y_2O_3 particles.

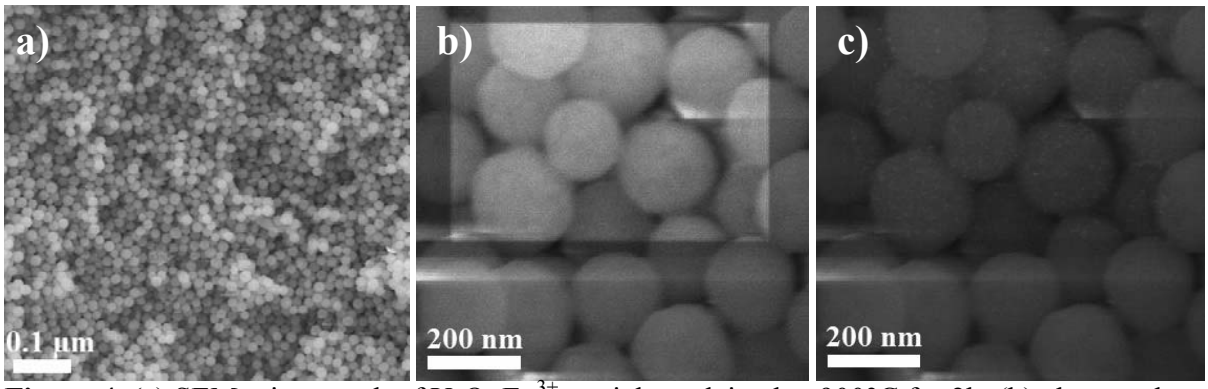

Figure 4. (a) SEM micrograph of Y_2O_3:Eu^{3+} particles calcined at 900°C for 2h, (b) elemental mapping of Y element (green color) and c) elemental mapping of Eu element (red color).

CONCLUSIONS

Monodispersed Y_2O_3:Eu^{3+} luminescent particles are obtained by microwave assisted urea precipitation method. Compared to conventional precipitation method the microwave-assisted method is a fast method (5 min to 30 min versus 2h reaction time) with a high batch-to-batch reproducibility. In microwave synthesis method increasing the reaction temperature, and consequently the reaction pressure, the efficiency of precipitation process is improved. The crystalline phase of calcined Y_2O_3:Eu^{3+} particles at 900°C is cubic Y_2O_3 and slight shift of the

peak positions to lower angles in XRD pattern confirms the presence of the dopant ions in the host crystal structure. These particles exhibit a strong red emission peak at 613 nm under the UV excitation (235 nm) due to the $^5D_0$–$^7F_2$ transition of Eu^{3+} ions in host matrix, which becomes more intense with increasing reaction time. The synthesized particles display spherical morphology and narrow size distribution, which are the key factors of bioimaging applications. Moreover the intense red fluorescent emission, excellent stability and low toxicity make these QDs promising for applications in bio-related areas.

ACKNOWLEDGMENTS

Adrine Malek Khachatourian would like to thanks Olle Erikssons foundation for the scholarship nr VT-2014-0001.

REFERENCES

[1] S. Zhong, J. Chen, S. Wang, Q. Liu, Y. Wang, S. Wang, J. Alloys Compd. 493 (2010) 322.
[2] W. Liu, Y. Wang, M. Zhang, Y. Zheng, Mater. Lett. 96 (2013) 42.
[3] S. Zhong, S. Wang, Q. Liu, Y. Wang, S. Wang, J. Chen, R. Xu, L. Luo, Mater. Res. Bull. 44 (2009) 2201.
[4] D. Dosev, B. Guo, I.M. Kennedy, J. Aerosol Sci. 37 (2006) 402.
[5] T.S. Atabaev, J.H. Lee, D.-W. Han, Y.-H. Hwang, H.-K. Kim, J. Biomed. Mater. Res. A 100 (2012) 2287.
[6] W.J.P. Ashutosh Pandey, M. K. Roy, Anjana Pandey, Marco Zanella, Ralph A. Sperling, and H.C.V. A. B. Samaddar, IEEE Trans. Nanobioscience 8 (2009) 43.
[7] C.A. Kodaira, A.V.S. Lourenço, M.C.F.C. Felinto, E.M.R. Sanchez, F.J.O. Rios, L.A.O. Nunes, M. Gidlund, O.L. Malta, H.F. Brito, J. Lumin. 131 (2011) 727.
[8] S. Mukherjee, V. Sudarsan, R.K. Vatsa, S. V Godbole, R.M. Kadam, U.M. Bhatta, a K. Tyagi, Nanotechnology 19 (2008) 325704.
[9] S. Mukherjee, V. Sudarsan, P.U. Sastry, a. K. Patra, a. K. Tyagi, J. Lumin. 145 (2014) 318.
[10] A. Boukerika, L. Guerbous, J. Lumin. 145 (2014) 148.
[11] N. Venkatachalam, T. Yamano, E. Hemmer, H. Hyodo, H. Kishimoto, K. Soga, J. Am. Ceram. Soc. 96 (2013) 2759.
[12] N. Venkatachalam, Y. Saito, K. Soga, J. Am. Ceram. Soc. 92 (2009) 1006.
[13] C. Traina, J. Schwartz, Langmuir 23 (2007) 9158.
[14] Y. Xiao, D. Wu, Y. Jiang, N. Liu, J. Liu, K. Jiang, J. Alloys Compd. 509 (2011) 5755.
[15] A. Malek Khachatourian, F. Golestani-Fard, H. Sarpoolaky, C. Vogt, M.S. Toprak, Ceram. Int. 41 (2015) 2006.
[16] D. Sordelet, M. Akinc, J. Colloid Interface Sci. 122 (1988) 47.
[17] G.S. Gowd, M.K. Patra, M. Mathew, A. Shukla, S. Songara, S.R. Vadera, N. Kumar, Opt. Mater. (Amst). 35 (2013) 1685.